

# Fabrication of Aluminum Surface Composites through Friction Stir Deposition

<sup>1\*</sup>Manoj Sarkar, <sup>2</sup>Neha Verma, <sup>3</sup>Rahul Kumar Gautam, <sup>4</sup>Sachin Rathore, <sup>5</sup>Kunwar Laiq Ahmad Khan

<sup>1</sup> M. Tech. Student, Department of Mechanical Engineering, KIET Group of Institutions, Delhi-NCR, Ghaziabad, AKTU Lucknow

<sup>2</sup> M. Tech. Student, Department of Mechanical Engineering, KIET Group of Institutions, Delhi-NCR, Ghaziabad, AKTU Lucknow

<sup>3</sup> M. Tech. Student, Department of Mechanical Engineering, KIET Group of Institutions, Delhi-NCR, Ghaziabad, AKTU Lucknow

<sup>4</sup> Assistant Professor, Department of Mechanical Engineering, KIET Group of Institutions, Delhi-NCR, Ghaziabad

<sup>5</sup> Professor, Department of Mechanical Engineering, KIET Group of Institutions, Delhi-NCR, Ghaziabad

**Abstract:**-Aluminum composites are commonly used in industries such as the aircraft industry, the automotive industry, the defense industry, the marine industry, and the automobile industry. Friction deposition was used to successfully create a composite of ceramic reinforcement particles. Layers were well-bounded, and extremely small in size grain, and the deposits were equally distributed and consisted of multiple layers of composite material. In this study, we use the friction stir deposition (FSD) approach to create an Al composite with the help of [Titanium diboride ( $\text{TiB}_2$ ) & yttrium oxide ( $\text{Y}_2\text{O}_3$ )] Pure aluminum powder is deposited onto a mild steel substrate utilizing an AA6063 consumable rod. AA6063 consumable rods were drilled with a variety of hole designs around their periphery. In this hole, we took 3 sample rods and drilled them with  $\varnothing 2.5$ ,  $\varnothing 4$ , and  $\varnothing 5.5$ -millimeter diameters for ( $\text{TiB}_2$ ) as well as 3 sample rods for ( $\text{Y}_2\text{O}_3$ ) ceramic particles. AFS-D deposits are investigated in terms of their macrostructure, microstructure, and mechanical properties, as well as their relationship to various process parameters. Analyses using a scanning electron microscope (SEM) showed that composite material was distributed more uniformly when 4 configuration consumable rods, such as  $\text{TiB}_2$  and  $\text{Y}_2\text{O}_3$ , were used. Equiaxed tiny grains were found throughout the composite's microstructure, indicating the existence of dynamic recrystallization during deposition. This treatment improves the material's base characteristics. Composites made from  $\varnothing 4$  of 4 holes of  $\text{TiB}_2$  and  $\varnothing 4$  of 4-hole  $\text{Y}_2\text{O}_3$  configurations were shown to have a longer plateau stress, which was a notable finding. Due to the material's uniform pore size, stress is gradually dispersed, increasing the material's toughness. Hardness was shown to have a non-linear relationship with  $\text{TiB}_2$  and  $\text{Y}_2\text{O}_3$  content at 4, thus, hardness rose up to a certain concentration but thereafter dropped. Thus, it is clear that precise modifications in  $\text{TiB}_2$  and  $\text{Y}_2\text{O}_3$  concentrations are required to produce optimal material characteristics, underscoring the significance of accuracy in composite formation.

**Keywords:** Aluminum composite; FSD; solid-state fabrication microstructure; tensile test; compressive test; Wear test, Scanning Electron Microscope (SEM), and Hardness Test.

## 1. Introduction:

Aluminum composites are widely used because of their lightweight, durable, and corrosion-resistant construction. They allow planes to carry less weight, which improves efficiency and performance. They are used in cars to make them stronger without making them heavy, which improves gas mileage. Alu-composite armor and weapons are widely used in the military sector for the same reasons. They are highly sought after by the

maritime sector due to their exceptional resistance to corrosion, particularly in saltwater conditions. Aluminum composites excel in these areas due to their long service life, high performance, and low weight have recently arisen as a completely new category of materials. They differ from regular materials in that they are exceptionally strong and stiff. The addition of ceramic particles to aluminum alloys has allowed for the development of a new class of engineered materials with a superior performance-to-weight ratio [1]. Researchers have found that particle-reinforced composites outperform unreinforced alloys when it comes to wear resistance [2]. Many wear studies on aluminum-MMC have concentrated on systems that include aluminum alloys enhanced with silicon carbide and alumina particles [3]. Each year brings a greater demand for lightweight materials that don't sacrifice durability. To address this issue, scientists have developed a wide variety of materials, including the composite metal matrix (MMC). Low volume, high tensile power, resistance to corrosion, excellent rigidity, stable behavior at high temperatures, reduced part weight, fewer heat-induced stresses, and the capacity to increase mechanical properties are only some of AMC's numerous attractive features [4-6]. Composite materials that consist of a ceramic or other element-reinforced aluminum matrix are known as aluminum matrix composites. The process of strengthening a composite by including ceramic or other components. To improve its qualities to an acceptable level, metal has been strengthened. Common reinforcement materials in AMC include SiC [7],  $\text{Al}_2\text{O}_3$ , [8]  $\text{TiH}_2$  [9], and graphite [10]. 6061-T6 was manufactured by utilizing FSP and composite (SiC+Gr) and (SiC+ $\text{Al}_2\text{O}_3$ ) particles with an average size of 20 m. According to the findings, the nugget zone (NZ) is composed of a homogenous distribution of SiC, Gr, and  $\text{Al}_2\text{O}_3$ . They found that the microhardness of the alloy of aluminum 6061-T6 surface hybrid laminate can be decreased while the resistance to dry slide wear is greatly increased through the addition of Gr particles with silicon carbide instead of  $\text{Al}_2\text{O}_3$  particles. It was shown that microstructures and micrographs were linked to microhardness and wear characteristics [11]. For their material creations, [12] generated MMC from FSP. This study set out to discover if a hybrid Al-based composite reinforced with a combination of SiC and MoS<sub>2</sub> particles could provide a self-lubricating and resilient to-wear surface. Tests proved that the processed zone's reinforcing particles were evenly dispersed and that the surface layer's bonds with the base material were strong. There are several potential options, but friction stir deposition (FSD) stands out because of its low cost and high safety [13-15]. Since it doesn't have the drawbacks of liquid-phase bonding, such as melting and solidifying, FSP is a more dependable and effective option. Friction Stir Deposition (FSD) involves pressing a rotating consumable stud onto a substrate, which generates heat and plasticizes the material due to the high frictional forces involved. The procedure consists of three stages. At first, the substrate is forced down onto the rotating stud, which causes the material to soften due to the high friction. A flash will form around the stud as the material is forced outward. A stable state is swiftly attained, characterized by constant forces, moments, and temperature. Once the parameters are reached, the operation ends, with translation ceasing, the stud retracting, and rotation coming to a standstill. The recrystallization of microscopic structures is triggered by thermomechanical action. The mechanical properties of a component can be locally altered by using this technique to adjust the thickness of the material [16]. There has been a lot of research on the possibility of using Friction Stir (FS) to produce high-hardness particle-impregnated metal matrix coatings. For our first experiment, we employed FS to incorporate SiC particles into AA6082 deposits. Next, we performed wear tests, analyzed the particle volume percentage in the deposits, and probed the surface for localized hardness [17]. Subsequent studies targeted perfecting the method of depositing titanium particles into AA5083. The microstructure of these deposits was fine and equiaxed, and the particle dispersion was excellent. Adding in reinforcing particles helped the deposits' mechanical resistance even further [18]. Friction Stirring (FS) has been studied extensively for its ability to induce microstructural changes. After FS, the microstructure is 33% more polished due to this procedure [19]. To achieve a high-quality composite, it is necessary to investigate other ways of introducing the composite mixture into the substrate. Figure 1. Illustration of the FSD strategy for surface composite development. Therefore, the purpose of this research is to evaluate the Friction Stir Deposition (FSD) method for creating a surface composite from ceramic powder, specifically titanium diboride ( $\text{TiB}_2$ ) and yttria-doped yttrium oxide ( $\text{Y}_2\text{O}_3$ ). The results of this study should help us better understand and utilize this technique in Aluminum surface composite manufacturing. In this study, the Aluminum composite is made by depositing, layer by layer, a disposable rod filled with a material onto the substrate. The features and prospective applications of the resulting surface composite are explained by in-depth characterization microscopy, scanning electron microscopy investigations, and tests for hardness, tensile, wear, and compressive behavior.

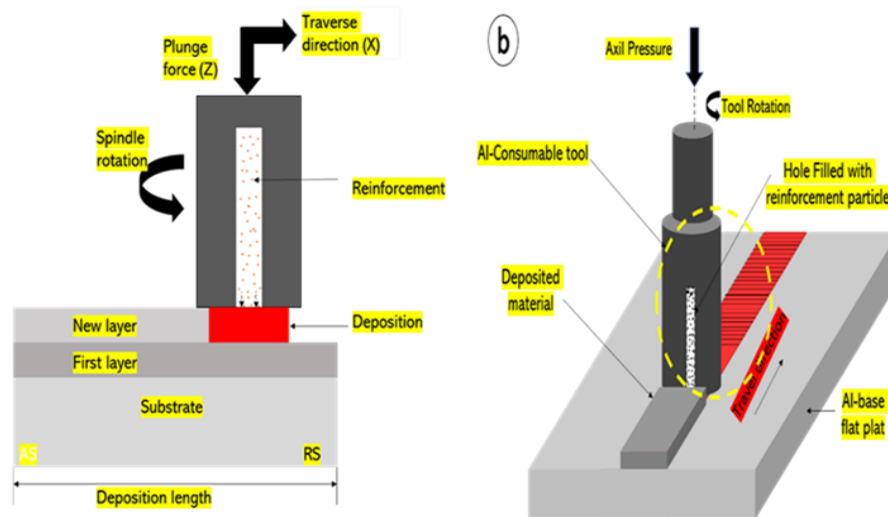


Figure1.Illustration of the FSD strategy for surface composite developed.

#### Procedure for Experimentation:

##### Components and operational settings:

The research began by selecting a mild steel (SS-304) substrate of 12 mm in thickness. In the deposition process, 25-millimeter in diameter by 80 mm long AA6063 consumable rods were employed. These rods were put on the substrate after being stuffed with a composite substance. A variety of holes, up to 30 mm in length, were drilled into the rods with a twist drill to introduce the composite mixture. Spectrometry was used to analyze AA6063 and determine its chemical makeup in this investigation. Table 1 shows that the concentrations of the alloy's constituents fall well within the acceptable range for AA6063. This verifies the high quality and credibility of the sources included in the study. Titanium diboride, or  $TiB_2$ , is a ceramic compound made up of one titanium atom and two boron atoms. Figure 2. Working on a semi-automatic milling machine. It is roughly 68.88% titanium and 31.12% boron in composition.  $TiB_2$  high melting point, electrical conductivity, and great toughness, as well as its resistance to wear and oxidation, make it useful in a variety of applications. The chemical formula for yttrium oxide, also called yttria, is  $Y_2O_3$ . It has two yttrium atoms (representing roughly 78.7 percent by weight) and three oxygen atoms (representing roughly 21.3 percent by weight). The high melting point and excellent stability of this white crystalline material have earned it a stellar reputation. Its high thermal and chemical stability makes it useful in a wide range of ceramic and electronic applications, particularly as a gate dielectric. The powdered AA6061 used for the base plate is chemically similar to the stabilizing agent used in the experiment. This optimizes material performance and cohesiveness across the board by ensuring compatibility and homogeneity between the base plate and the stabilizing agent.

Table 1. Aluminum 6063 Composition

Al	Si	Fe	Cu	Mn	Mg	Cr	Zn	Ti
99.60%	00.25%	00.35%	00.05%	00.03%	00.03%	00.05%	00.05%	00.03%

Titanium diboride ( $TiB_2$ ) and yttrium oxide ( $Y_2O_3$ ) were used as the blowing agent for the experiment. The chosen blowing agent has a purity of 95.5+%, 99.99%, and a mesh size of 200,325. Powders made up of  $TiB_2+Al$  and  $Y_2O_3+Al$  were mixed in at a weight ratio of 50:50. This combination ensured a well-rounded and efficient composite mixture, just right for the task at hand. The components were distributed evenly throughout the mixture because of the thorough mixing. There are six distinct types of sample rods, each of which has a different number of holes for ( $TiB_2$ ) and ( $Y_2O_3$ ), ranging from 2.5, 4, and 5.5. The width of the holes bored into the consumables rod was carefully chosen to keep the volume of the ceramic material used per unit of length of

rod consistent. In order to get good coverage of material when depositing, the locations of the holes around the rod's perimeter were selected by trial and error. Positioning these holes carefully avoided weakening the rod in any one direction, which may have led to uneven deformation or dispersion of the composite mixture during deposition. When there were seven or more holes instead of six. This was learned through experimental trials. Because of this imbalance, the structural integrity of the material was weakened, and as a result, it lacked the necessary robustness to hold on to the ceramic powder in a consistent manner throughout the deposition process. Figure 3. is a diagrammatic representation of a consumable rod that has holes that have been bored.

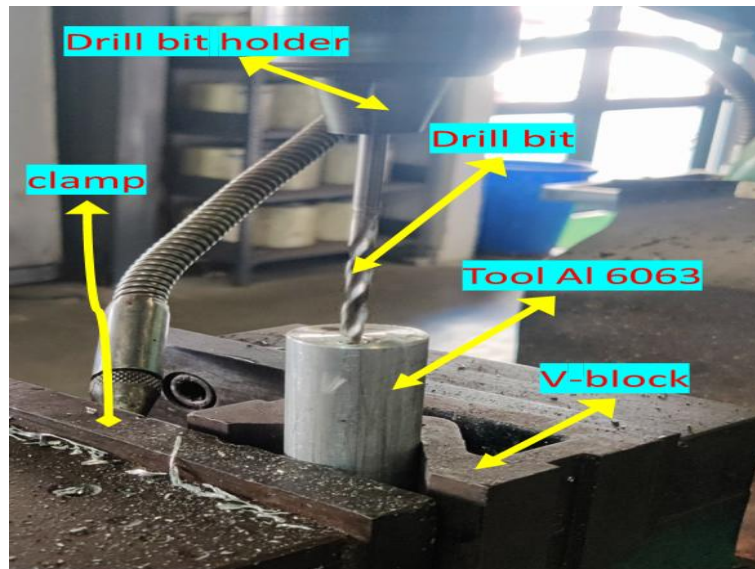


Figure2.Working on a semi-automatic milling machine

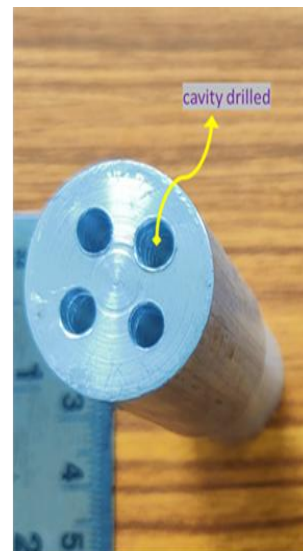
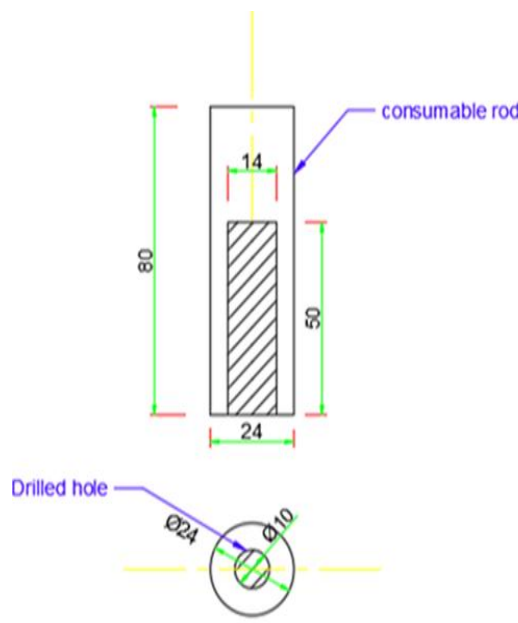


Figure 3.Schematic illustration of the disposable rod and Images of the rod after drilling.

Designation	Top View Dim (Consumable Rod)	Side View Dim (Consumable Rod)
-------------	-------------------------------	--------------------------------



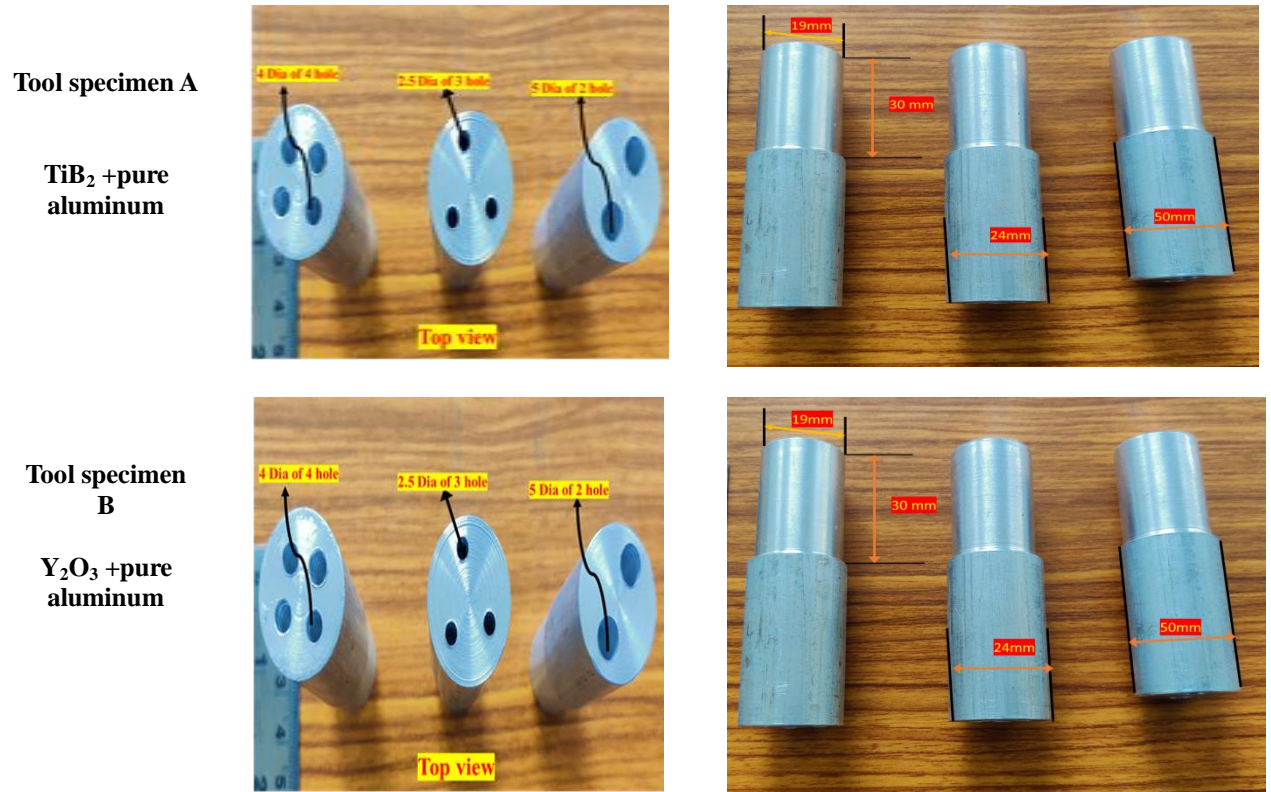


Figure 4. Drilled rod in its original form.

In Figure 4, you can see the initial photographs of the consumable rods after the holes were prepared. These pictures are from before the holes were prepared. The process for filling composite mixtures is done in phases to guarantee that the mixture is completely and uniformly filled over its whole length with no gaps for air to pass through. Figure 5. Details of specification of reinforcements powder and original rod Then, Silver foil paper, available for purchasing in the market, is used to seal the ends of the pores after the mixture has been inserted to prevent any of the combinations from leaving before the deposition process begins. In scientific experiments, it is common practice to expand upon previously gathered information. It is stated that "Other experimental process parameters are identified based on previous research when more primary reinforcement is added, the fundamental qualities improve, and when secondary reinforcement is added, the composite properties are achieved [20]. This method assures that the experiment is based on reliable information by drawing on previous studies. This builds on the work of others and lends more weight to the experiment, increasing the odds that it will be successful or optimized [21-25]. It implies that the current study's parameters were not chosen at random but rather were affected by past studies [26].

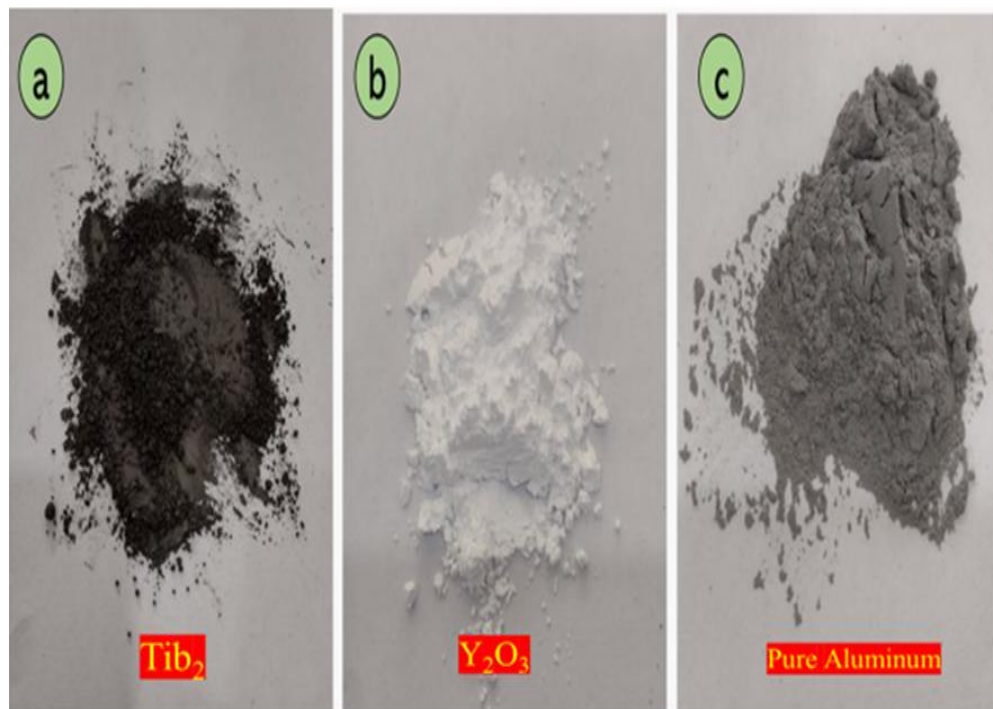


Figure 5. Details of specification of reinforcements powder and original rod.

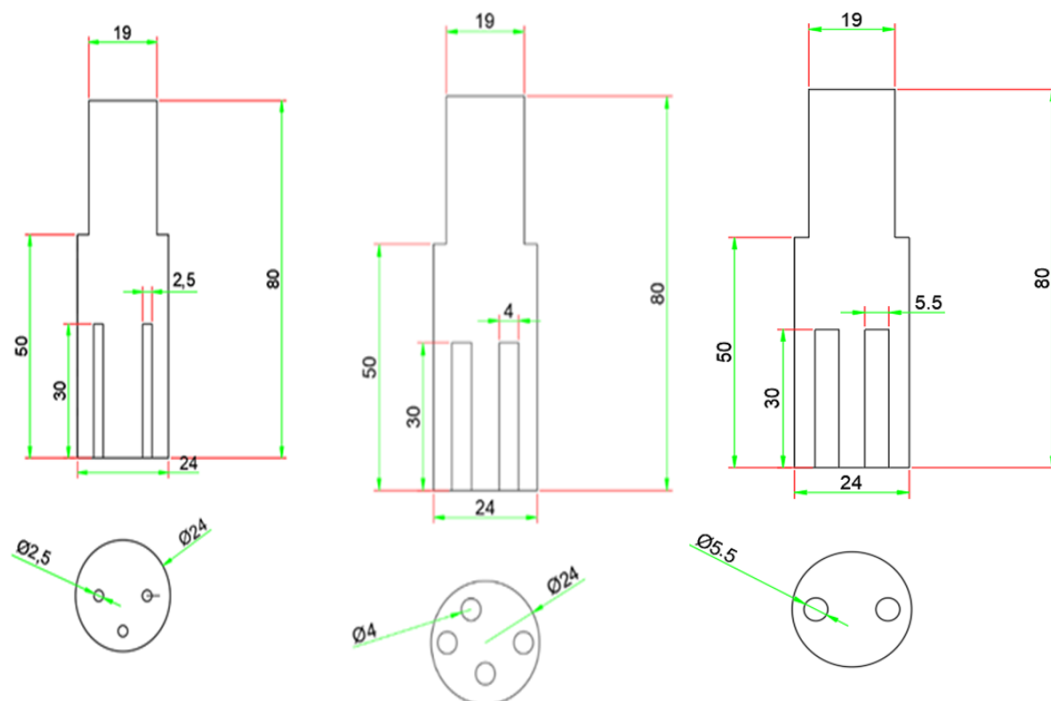


Figure6. Schematic illustration of the disposable rod

Table 2 shows the Consumable rods of a 24 mm diameter utilized in conjunction with a steel substrate plate in the Friction Stir Deposition (FSD) research for AA6063. Unique to this study was an examination of how changing the rod hole design affected the final surface composite consistency in terms of mixing uniformly. The purpose of this research was to establish a causal link between hole style and performance and the qualities of the Aluminum composite produced by treating the hole design as the main variable while holding all other process factors constant.

Table 2.Modifying the process's variables based on the rod's profile and material makeup

Designation	Holes in rod	Rod Dia (mm)	Rotational speed (RPM)	Feedrate (mm/min)	Mixer composition
Tool specimen 1	2.5	24	2000	20	50% TiB <sub>2</sub> + 50% Pure Al powder
	4	24	2000	10	50% TiB <sub>2</sub> + 50% Pure Al powder
	5.5	24	2000	10	50% TiB <sub>2</sub> + 50% Pure Al powder
Tool specimen 2	2.5	24	2000	20	50% Y <sub>2</sub> O <sub>3</sub> + 50% Pure Al powder
	4	24	2000	10	50% Y <sub>2</sub> O <sub>3</sub> + 50% Pure Al powder
	5.5	24	2000	10	50% Y <sub>2</sub> O <sub>3</sub> + 50% Pure Al powder

#### Tensile test flat-type specimen:

In tensile testing, the standard flat-type specimen is a long, uniform strip with a uniform width along its length, which is where most of the measurements are collected. Figure 7, Schematic representation of the surface composites used to create the test specimens This part in the middle is the most vulnerable to necking and subsequent fracture. The specimen has wider ends where the testing machine can grab a firm hold of it. The gauge length, critical for stress analyses, is marked on this piece. When testing for notch sensitivity or impact resistance, notches may be present on the specimens used. Specimens of materials with directionally dependent characteristics, such as some metals and composites, may be labeled to indicate their orientation concerning the grain or rolling direction. The ASTM-E8/E8M-16a standard was used for all of the tensile tests, and the tests were tested using an Instron tensile machine at room temperature and with a fixed working tip rate of 2 mm/minute.

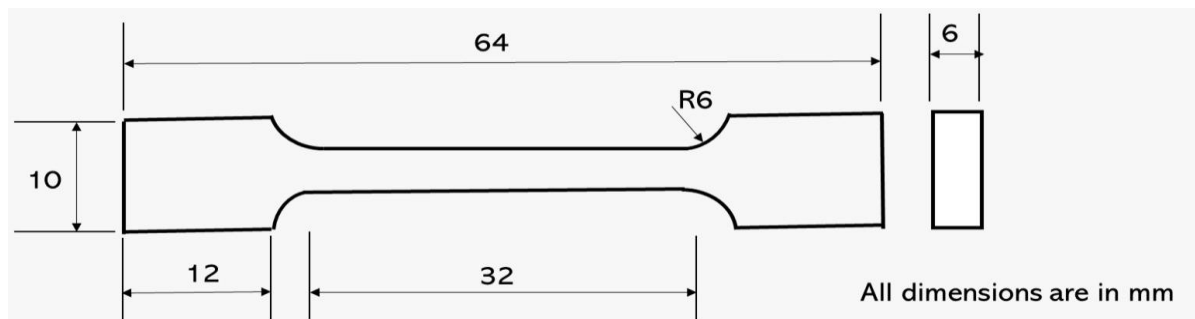
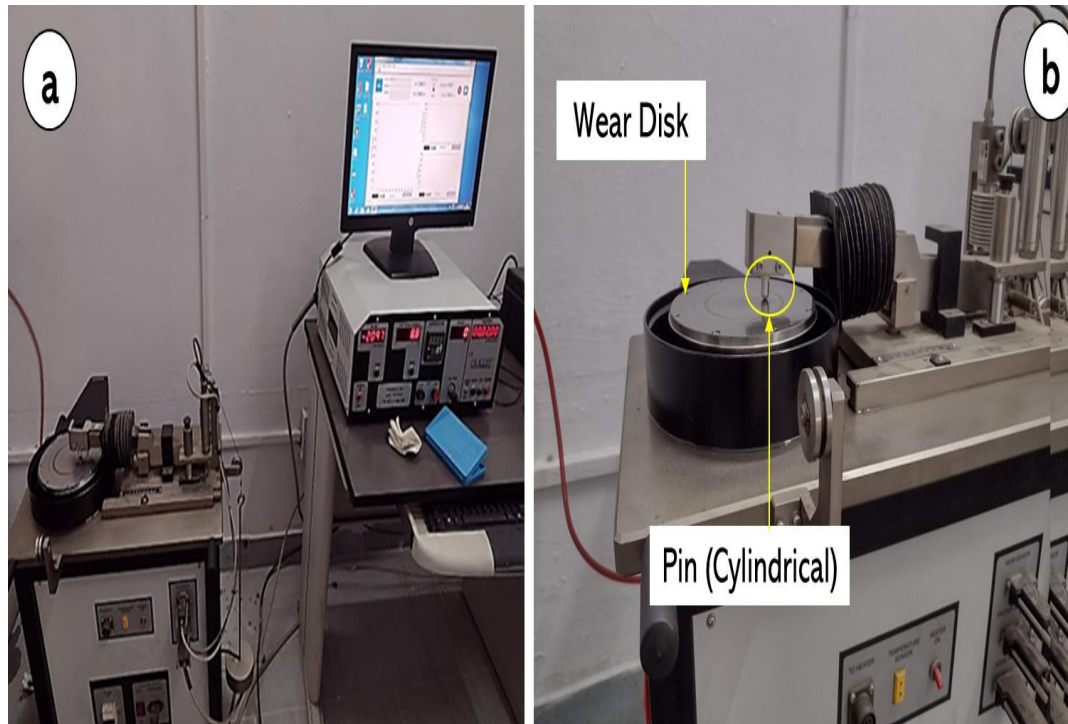


Figure 7. Schematic representation of the surface composites used to create the test specimens.

#### Wear testing equipment:

The pin-type wear test involves pressing a pin (or sometimes a ball) against a rotating disk. As the pin, symbolizing the material being evaluated, glides or rolls across the surface, it wears down due to friction. After a predetermined amount of time, the test is stopped, and the pin's wear is evaluated (usually by measuring its decreased mass, expanded dimensions, or microscopic wear scars). Figure 8, Displays the experimental

configuration for pin-on-disc wear testing. Modifying variables like sliding speed or temperature allows the test to replicate a wide range of real-world situations, whether dry or lubricated. The information helps make decisions about which materials to use and how to increase their resistance to wear.



**Figure 8. Displays the experimental configuration for pin-on-disc wear testing.**

Pin-type wear testing is a straightforward approach to learning about a material's wear properties. Industries such as automotive, aerospace, and manufacturing rely heavily on the results of such testing due to the importance placed on material durability and performance under frictional contact.

### Methodology of Depositions

At first glance, the AFSD machine may look like a configuration used for fused deposition modeling (FDM), a technique often utilized for printing thermoplastic using heat and compression. Metal deposition, on the other hand, places stringent requirements on the process, particularly in terms of material deformation and establishing a strong bond with the substrate. As such, AFSD makes use of the friction stir principle. In conjunction with a vertical feed mechanism, this method allows for the "printing" of metals by rapidly heating and deforming them, resulting in efficient deposition and robust adherence. The procedure is complete once the mixer-filled rods are deposited onto the substrate in a layer-by-layer fashion, which is illustrated in Figure 9 (a-d). In AFSD, the metal rod spins rapidly, generating heat where it contacts the substrate through friction. The feed material is heated and softened so that it can be extruded between the base material and a spinning tool head. When the tool is rotating, the bottom edge of the head smears and shears the deposited layer to remove any air bubbles and set a limit on the layer thickness. The co-deformation of the deposited substance and the substrate during this process creates an extremely strong link between the two.



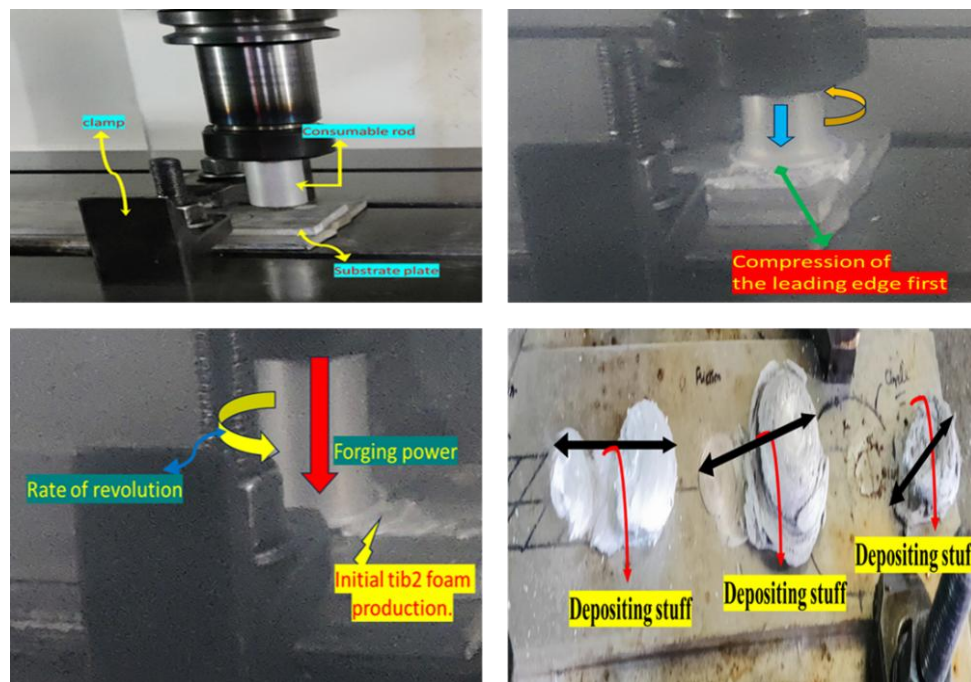


**Figure9.a)Frictional deposition of AA6063, b) Initially diving down, c) Deposition, d. Material that has been deposited**

The rods with the mixture inside were deposited stacked one by one onto the substrate, as shown in Figure 9, to create the aluminum composite. The deposition is carried out using a standard vertical machining center (PX 40 the VMC PX Series) equipped with location control of the work surface equipment's three axes and a motor producing 8.25 kW at speeds that vary between 35.5 to 6000 rpm. Table 3: Specifications of common CNC milling equipment. The experiment involves depositing a composite material onto a steel plate by driving an aluminum rod filled with the mixture into the plate and then feeding it along the plate's surface at a velocity of 40 mm per minute.

**Table 3. Technical details about CNC milling machines.**

Type of machine	Vertical machine center
Machine	PX Series VMC PX 40
Table size	915 x 460 mm
Spindle motor capacity	8.25 kW
Rapid feed traverse (X, Y & Z Axis)	25 m/minute
Spindle speed (max)	6000 rpm
Cutting feed	10 mm/minute
Positional precision	00.01 millimetre
Persistence accuracy	00.005 millimetre

During rubbing, the rubbing contact is transferred to the surface of the substrate. An interdiffusion process that is driven by pressure and heat creates a secure link between the components, and dynamic recrystallization creates a fine-grain microstructure in the material. As shown in Figure 9c, by gradually wearing down the consumable rod, FSD enables the creation of a continuous deposit. The illustration clearly shows this. In addition, as seen in Figure 9d, a revolving burst of viscoplastic material forms continuously at the rod tip during the process. The smooth mushroom-shaped disruption on the disposable rod was caused by this flash[26].

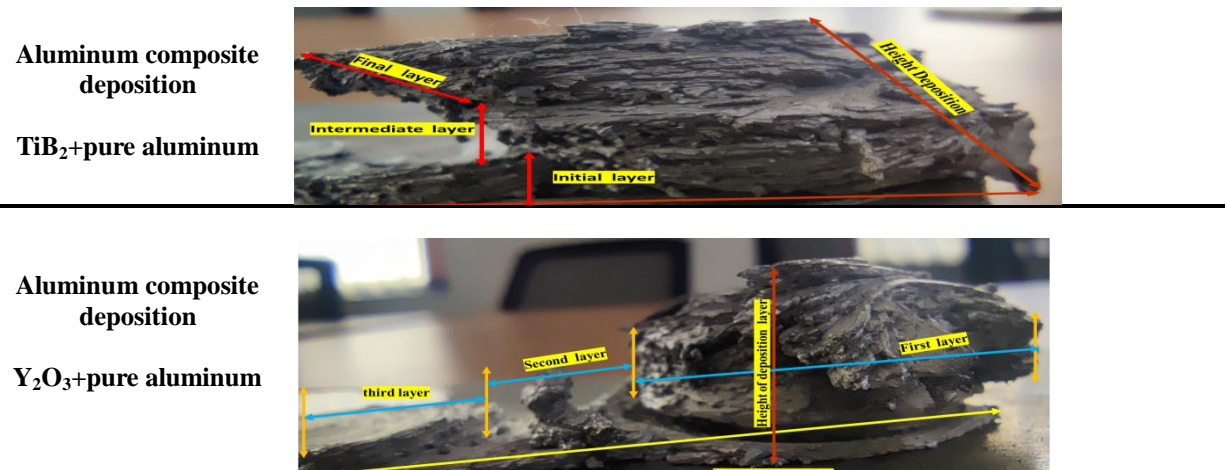


Figure 10. (a & b) Layer-by-layer deposition with FSD.

Figure 10 (a-b) illustrates the deposits that are generated by FSD when the process parameters are held constant. The curve wave markings point in a clockwise direction and indicate the direction in which deposits should be made by the consumable rod. As a result of the FSD process, wave markings will always be present on the surface of the deposits. This is an inherent property of the process. How material is transported is connected to the roughness of the surface as well as the formation of wave markings. The plasticized metal is put in several layers, each with its unique elliptical pattern, to create the desired effect. This demonstrates that the union process of the substrate proceeds from the side that is advancing to the side that is receding. The appropriate height and length of the deposits are achieved in every method for mixture filling hole profiles that are represented by a red line. This is evidence that the substance in question is bound to the substrate appropriately.

#### Composite production technique:

The substrates are taken from each FSD zone after the deposits are formed. composite (about 12\*12\*12 mm in size) is collected at the beginning, middle, and conclusion of each experiment, as shown in Figure 11. These spots were picked to ensure that the mixture was spread evenly across the FSD area., by rapidly rotating a metal rod as it is fed through the tool head, AFSD creates frictional heat as the rod makes contact with the substrate. Between the substrate and the revolving tool head, the feed material heats up, yields, and extrudes to fill the available volume. The tool's head has a dual-purpose bottom surface. As a first step, it acts as a vertical limit that regulates layer thickness. Because of its rotation, the deposited material is smeared and sheared even more, guaranteeing a smooth, pore-free print. When the deposited material and the substrate surface are co-deformed and mixed, a strong bond is formed at the contact. There are four distinct phases to the FSD of composite materialsthe beginning of friction, the material's plasticizing, the depositing process, and the end of the procedure. In the initial stage, friction onset occurred when the revolving consumable rod made contact with the substrate surface, friction that occurs between the revolving AA6063 consumables rod and the stationary substrate causes a significant increase in the measured load. Second, while the product rod and substrate were being stirred at a steady feeding rate, enough frictional heat was created to firm up the material and put it on the first coating layer. The recorded load instability at this point suggests that we may be in a transitional phase of the FSD process. The third phase involves constructing composite materials in uninterrupted layers from the bottom up over a predetermined amount of time while under a nearly constant recorded load. The durability of

the raw materials used to create the consumable rods ultimately dictated how they would perform during the FSD. Constant feed rates, rotational speed, and consumables rod volume showed that the AA6063 matrix composite's hard material displayed outstanding resistance to friction agitation. Figure 12. After the cutting process, the piece goes through the lathe to be faced as a result, AA6063 required more time to construct continuous layers. When the deposition procedure is complete, the revolving rod leaves upward, drastically reducing the deposition load.

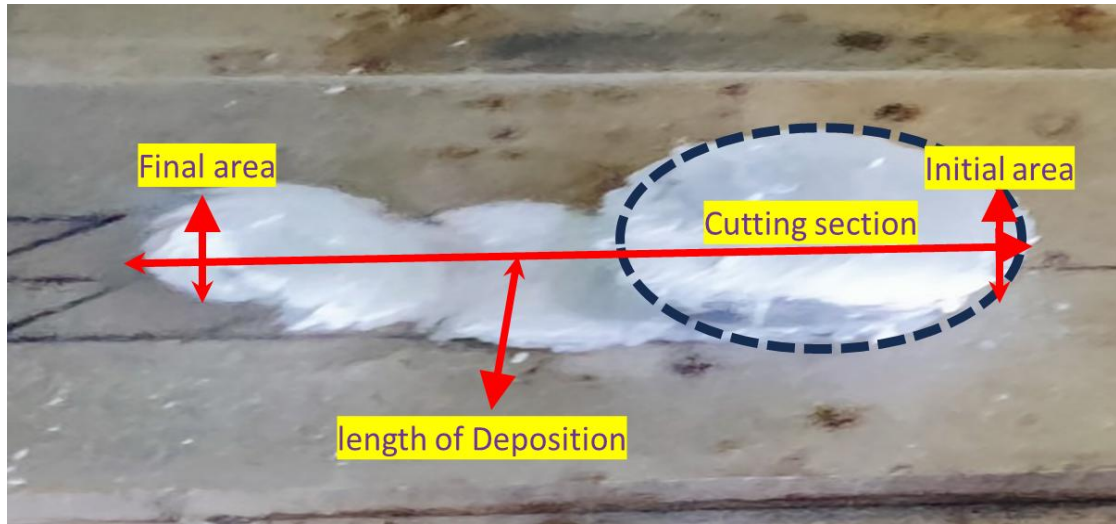


Figure11. Collection of FSD region samples.

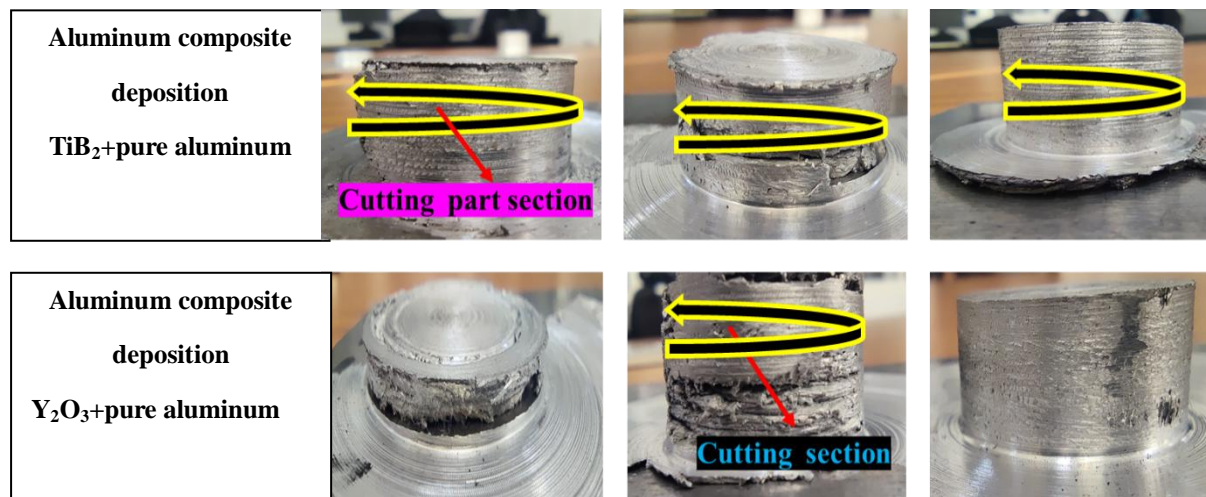


Figure 12. After the cutting process, the piece goes through the lathe to be faced.

#### Characterization:

Scanning electron microscopy (SEM), in particular the JSM-6510 model, is used for a detailed examination of the microstructure within the AA6063 composite material. The composition of the substance and the dispersion of the composite can be determined with the use of these instruments. To produce a glossy finish, the retrieved samples are polished using abrasive sheets of varied grit sizes. When the samples are etched with a variant of Keller's reagent, the larger structure of the coated material becomes visible. During Friction Stir Deposition (FSD), the quantity of heat produced is measured and tracked using a K-type thermocouple and Exttech (SDL200) data-collection device. The homogeneity of the composite agent in the treated zone is evaluated by analyzing the macrostructure and microstructure of AA6063 surface composite using microscopy. After etching a specimen with a variant of Keller's reagent, the treated zone's macrostructure becomes visible. In all



macrographs, the material flows from the initial side (IS) to the Final side (FS), as calculated by the pore size distribution of the produced composite sample using the software "ImageJ". Because of the directional nature of the tool stirring, materials can only move in one direction. It can be shown that there is no macro-segregation in the treated zone when using the technique and that the composite mixture is distributed uniformly. Materials' responses to a compressive load can be evaluated through a technique called compression testing. The ability of a material to bear compressive loads or reductions in size is measured by this type of test. The tensile test is a common mechanical procedure used to evaluate a material's strength under tension. In summary, Table 4. The Vickers micro-hardness tester (made by Omni tech Mvh1, India) was used to measure the microhardness of the deposited and base materials, and the results showed that the load of 0.98 N applied for 20 seconds gave accurate results. Wear resistance can be objectively assessed with the Pin-on-Disc Testing Machine. The disc speed and pin load are adjusted after initial measurements and cleaning of the pin and disc samples. Environmental controls are a common aspect of modern equipment. Modern machines automatically capture important data during testing, during which the pin's travel on the rotating disc forms a wear track. Microscopical inspection of the worn area after a test is performed to determine wear metrics for comparison. Insights into the material's wear characteristics and applications are gained through this analysis, guaranteeing accurate comparisons between materials. A tensile test is a standard mechanical procedure in which a sample is stretched until it breaks. The main goal is to calculate the mechanical characteristics of the material, like its tensile strength, yield strength, and elongation. A specimen is clamped at both ends and stretched using a machine that exerts a progressive force during the test, with the shape and size of the specimen being standard. A stress-strain curve is generated by measuring the force exerted (stress) and the amount by which the specimen is deformed (strain) when it is stretched. The results of the test can help inform decisions about which materials to use and how to design those materials for certain purposes.

**Table 4. Observation table for compression testing of all surface composite.**

Sample	Type	Diameter	Thickness	Position
4 holes-4 Dia	$Y_2O_3$ + Pure Al	23.43	6.58	stand type
4 holes-4 Dia	$TiB_2$ + Pure Al	20.44	5.67	stand type

### The Outcome and Discussion:

Several tests were done to see how the consumable rod behaved so that the rotating rod wouldn't buckle during the FSD process and to make sure that the layers of the aluminum mixtures kept being added without any visible flaws. The FSD process was then used to make the AA6063 aluminum composite for temper conditions, with a size of 24 mm. A feeding rate of 10 mm/min and a rotation rate of 2000 rpm were chosen as the best processing conditions for making an aluminum laminate in this study based on the results of these tests. The used-up AA6063 consumable rods and the deposited materials are depicted in Figure 13. At a speed of rotation of two thousand revolutions and an input rate of 10 millimeters per minute, the aluminum composites were effectively produced within the tempering parameters of the starting consumable rod AA6063.

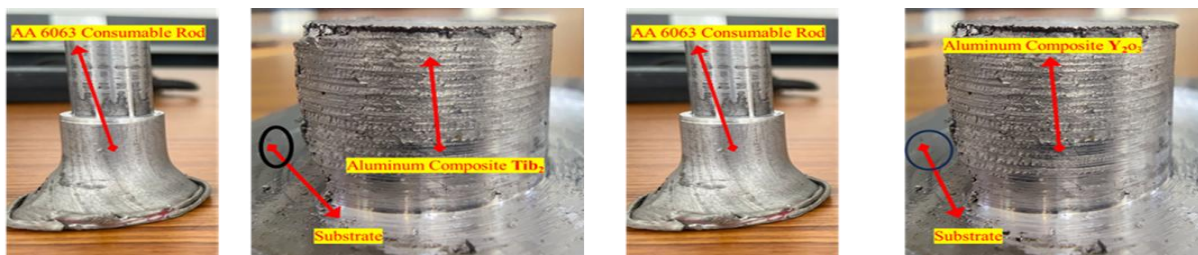


**Figure 13. Images of the AA6063 aluminum composite  $TiB_2$  and  $Y_2O_3$  deposited at two thousand revolutions per minute rotation speed and 10mm/min feed rate for additive manufacturing.**

The literature evaluation reveals that no studies elaborate on the steps involved in deposition when making Al-based composites using FSD. The deposition load value displayed in the present work's monitoring for the FSW/FSP machine can be used as an indicator for the resistance of consumables rod materials that are put on the substrate plate, which depends on the as-received material. Matrix loads applied during FSD testing of AA6063 composites, and their corresponding stages.

### Examination of the deposit zone using a macrograph

#### Scanning electron microscope (SEM)

SEM analysis of rods with a variety of mixture-filled hole profiles was used to look into the microstructural differences in the deposition zone. [Sem] microscope analysis led to the selection of two-hole profiles (each with four holes) for further study of the microstructure and flow patterns of the deposited material. The results of the SEM examination agreed with those obtained using the microscope. Micrographs taken with a scanning electron microscope reveal that the distribution of particles is very sensitive to the number and size of holes. The Macrostructure of ASCPs produced at AA6063-T6 temperature conditions, 2000 rpm rotation speed, and 10 mm/min feed rate is shown in figure 14a. shows macrostructure of cross-sections of deposited ASCs showing entirely continuous structures without bonding holes and flaws. SEM pictures also show that particle dispersion is affected by factors such as hole size and number, specifically for 4-hole types ( $\text{TiB}_2$  AND  $\text{Y}_2\text{O}_3$ ). Having more holes means more surface area is available for distribution during deposition, vastly improving mixture dispersion. Defect generation is also seen to be more likely when there are more holes in the deposition rod. According to the SEM results, crack-like flaws appear in the DZ when the number of holes exceeds five.

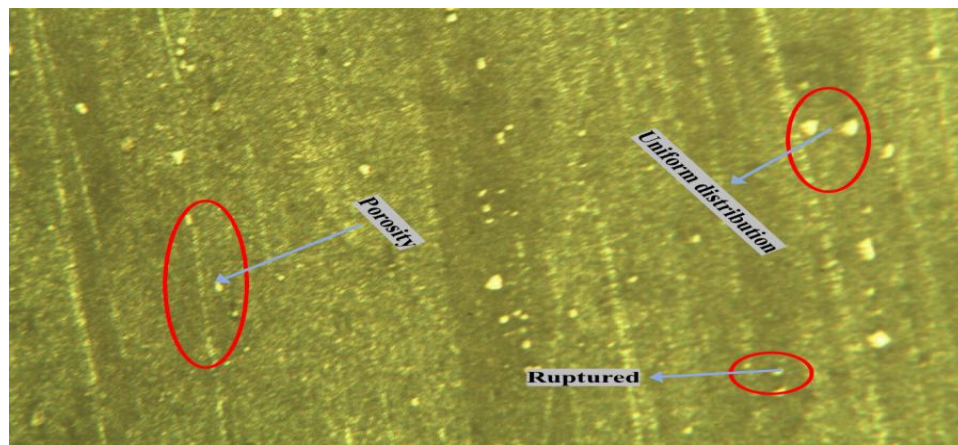


Figure 14. (a) Composite  $\text{TiB}_2$  as-received Scanning Electron Microscope (SEM-SE) picture consumable tool



Figure 14. (b) Composite  $\text{Y}_2\text{O}_3$  as-received Scanning Electron Microscope (SEM-SE) picture consumable tool.



The depicts a deposited section of a four-hole rod profile after FSD, which is used to study the deposit's microstructural development. Three portions, one from the leading edge, one from the middle, and one from the trailing edge, are selected to examine the rod's microstructural development at various stages of processing. The microstructure of the consumables material (AA6063) received is shown in Figure 14(b). The thermomechanical changes that occur to the consumable rod during processing make the deposited material finer in grain size. The grain size varies just slightly between the first (IS) and last (FS) layers of deposition in the depicting fine-grain morphology. Refined grains' signature microstructure results from the deposit property of heat and deformation, which permits the dynamic reconstitution of the material. During this process, the first collection of distorted particles gives the appearance of a collection of new equiaxial particles.

#### Microhardness profile of Al Surface composite:

As received, the AA6063 consumables rod (primary substance) has a hardness of 76.04 HV. Microhardness profiles for each FSD condition were measured using a disposable rod with four-hole profiles, as shown in Fig. 15. As can be shown the deposits created using a rod with four holes had hardness values from 40 and 51 HV. Figure 16 hardness values were analyzed longitudinally to determine the quality of the deposits. Four-hole profile sample (a) from the deposit, showing (b) the as-received structures rod, (c) the advancing side microstructure, (d) the middle section microstructure, and (e) the side that re-treats microstructure from left to right at 0.5 mm intervals.

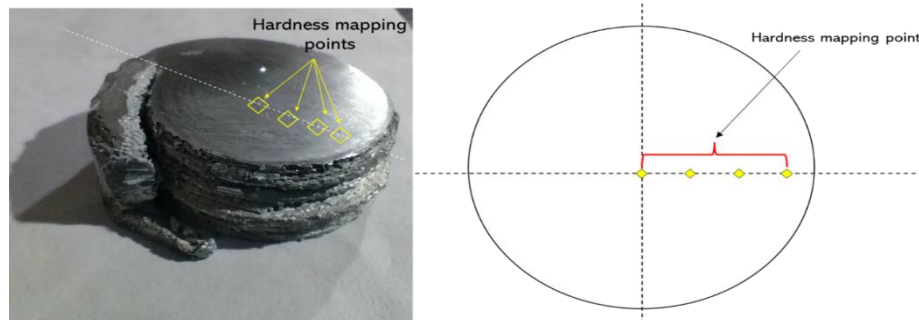


Figure 15. Microhardness profile of the aluminum surface composite material.

The deposits have a lesser hardness than the consumables rod in its as-received state. The heat produced during the process causes the levels of hardness in the deposits to drop more precipitously in the central region, allowing grain deformation to regenerate and reorganize in the direction of roll. Since hardness is a direct function of microstructure, this may have an effect on the values here [27]. The data demonstrates that the hardness levels across all six processing scenarios are extremely similar. The degree of hardness levels in each deposit may vary due to a number of reasons, including microstructure and the existence of faults, although these differences may also be due to chance.

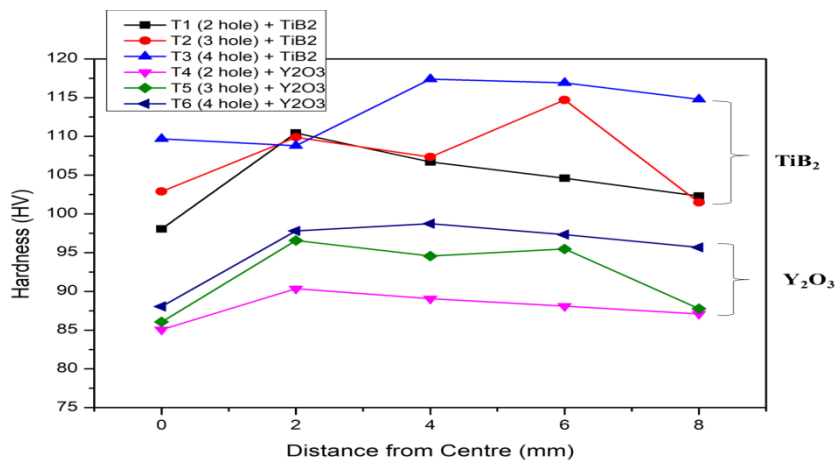


Figure 16. Al Surface composite hardness variation along the zone of processing.

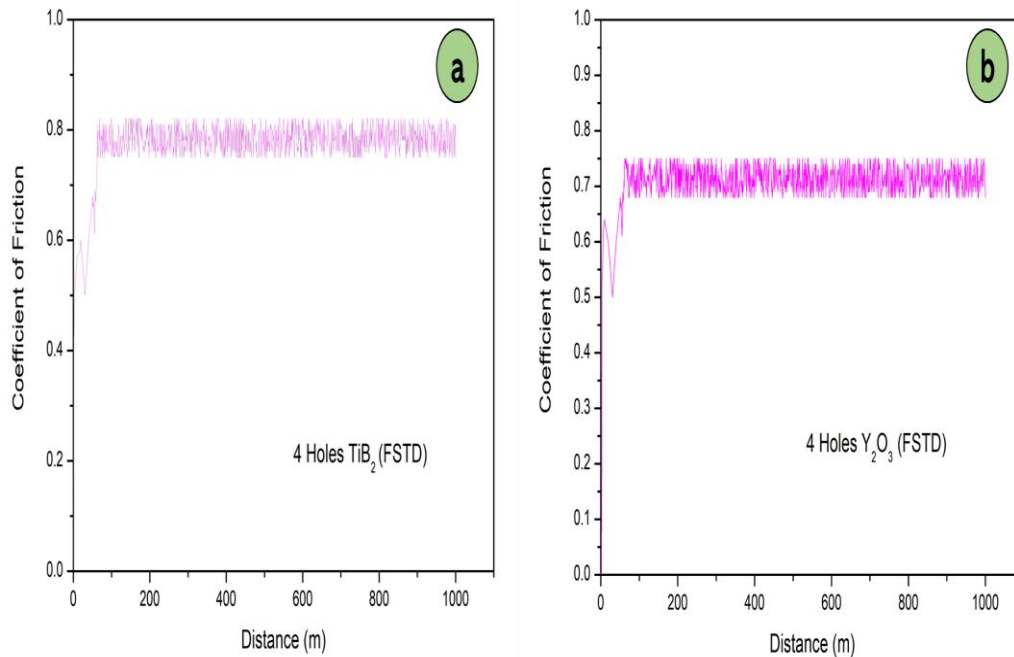
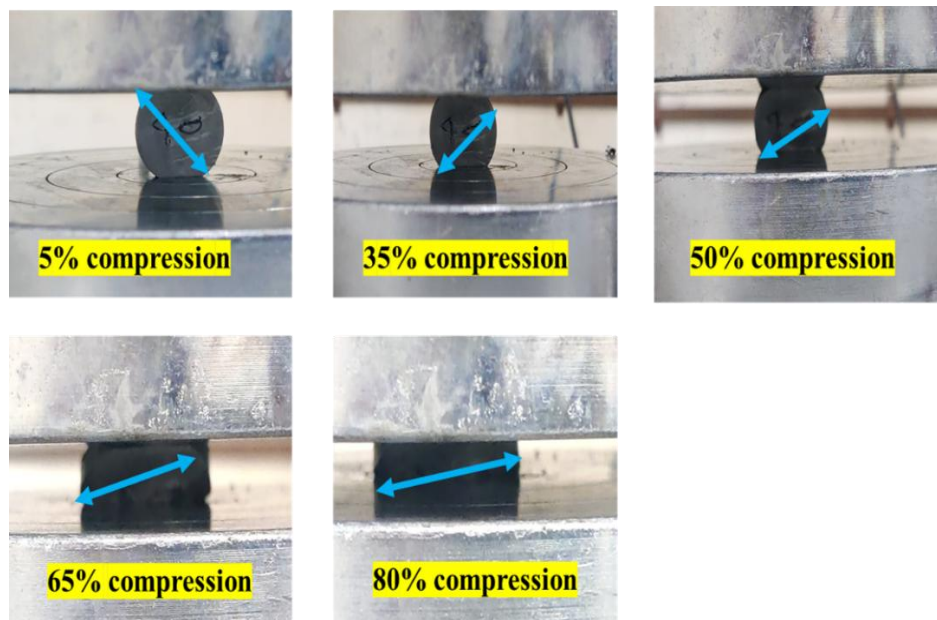


Figure17.the surface composite test used to generate the coefficient of friction vs. distance (m)

#### Compression test of developed surface composite:

The most common type of mechanical testing is compression testing, which is used to assess the compressive behavior and absorption of energy capability of composites. To study the stress-strain relationship, we performed a compression test with a fixed strain rate of 1 mm/sec. There are three distinct phases of deformation visible in compression tests. The first stage of deformation is more rapid because of the initial tension required for structure deformation. As the surface composite deforms, strain rises without a matching increase in tension in the second phase, which is a constant deformed zone. This plateau stress is used to characterize the energy-absorbing properties of composites during compression. The third phase, densification, results in a cumulative increase in stress and strain. Figure 18. Compressive surface composite deformation, from (a) 5%, (b) 35%, (c) 50%, (d) 65%, and (e) 80%. The initial stage of a four-hole composite is fairly shallow, but the second stage's steepening slope indicates that the composite is becoming denser as strain increases. Rods with Ø4 holes of  $\text{TiB}_2$  and 4 holes of  $\text{Y}_2\text{O}_3$  produce a composite with a wide plateau zone that shows persistent composite deformation. Four-hole type AA6063 FSD ( $\text{TiB}_2$  and  $\text{Y}_2\text{O}_3$ ) [489.7 MPa] strength of compression and strain are shown to be lower than those of ASC specimens (Ø2.5, Ø5.5 & Ø2.5, and Ø5.5). The incorporation of  $\text{TiB}_2$  greatly enhanced the AMCs' resilience to deformation. At strains up to 57.7%, no cracks appeared in ASCs of varying  $\text{TiB}_2$  concentration. With strains between 5% and 34%, the compressive force of the Ø4 is greater than that of the AMC samples (Ø2.5, Ø5.5 & Ø2.5, Ø5.5), demonstrating that the work-hardened coefficient of the number (n) of the 4-hole type is bigger.  $\text{TiB}_2$  and  $\text{Y}_2\text{O}_3$  enrich the ASC samples, which in turn raises their "n" value. This boosts the ASCs' compressive strength as an added bonus. In comparison to the compressive strength of Ø4, which is 489.7 MPa, the compressive strength of Ø5.5 is 834.4 MPa, an increase of 78.5%.



**Figure 18. Compressive surface composite deformation, from (a) 5%, (b) 35%, (c) 50%, (d) 65%, and (e) 80%.**

#### **Composite surface wear analysis:**

Pin and disc specimens are cleaned to remove any impurities and their initial size and weight are documented before the test. After the machine has been unpacked, the disc is placed on the revolving platform and the pin is oriented so that it will touch the disc's surface. It is calibrated such that the force applied by the pin to the disc is constant throughout the test. Set the rotational speed of the disc and the total distance to be slid (or the duration of the test), and then start the test. The pin wears out from rubbing against the spinning disc because of the sliding action. Modern machines can automatically record crucial characteristics like frictional force, allowing for an instantaneous evaluation of the coefficient of friction. When the specified amount of time has elapsed, the machine is turned off and the samples are carefully removed for further examination. The pin's post-test measurements or weight are measured, and the wear scar and disc wear track are inspected to determine the level of wear. Data, results, and any unusual occurrences during testing are recorded precisely. Under controlled conditions, this method provides an in-depth understanding of the wear and frictional properties of a material.

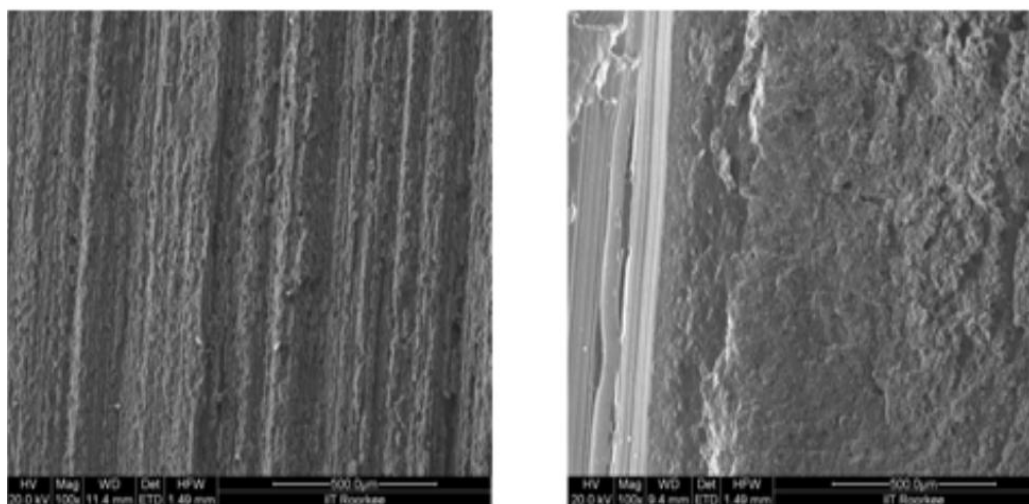


**Figure 19. Scanning Electron Micrographs of (a) a Carburized Sample Wear Track (b) a wood pi with a wear scar.**

Wear resistance decreases with an increasing proportion of reinforcing compared with base alloy, as determined by a number of investigations [28,29,30]. This is because, as the level of load increases, the reinforcements reduce the wear rate to a minimum [31]. A higher coefficient of friction is one of the benefits of increasing the reinforcing content in the base alloy [32]. The wear track in Fig. 5 is rather even, and there is relatively little debris. Surface composite samples show less weight loss due to wear because of their higher density (compared to gravity-composite samples) which prevents particle pullout and thus wear. Harder materials mean less wear weight loss and Aluminum surface composite samples with a higher density show this by being less deformed on the surface during a hardness test.

#### Tensile test of surface composite:

A flat specimen type was created, and then it was held firmly between the grips of a testing machine to perform a tensile test, a standard. The tensile test is a vital tool in metallurgy, manufacturing, and quality control, offering insights into a material's ductility, elasticity, and strength. The machine applies a force on the specimen and gradually increases it. Real-time measurements of the applied load and the amount of deformation of the specimen are taken and stored. A stress-strain curve is created from the data to graphically display the material's tensional behavior. Temperature and humidity control are additional variables that must be adjusted in some studies. (UTS), (HV) and (SZ) are summarized in Figure 20. As seen in Fig., UTS improves with more passes and reaches its optimum at a constant spindle speed of 1000 rpm. These factors have contributed to UTS's growth and development. Matrix grain size is decreased by the use of multi-pass FSP due to the smaller cluster size and more even dispersion of reinforcement particles [33]. Second, the dispersion of reinforcements causes a decrease in porosity [34].

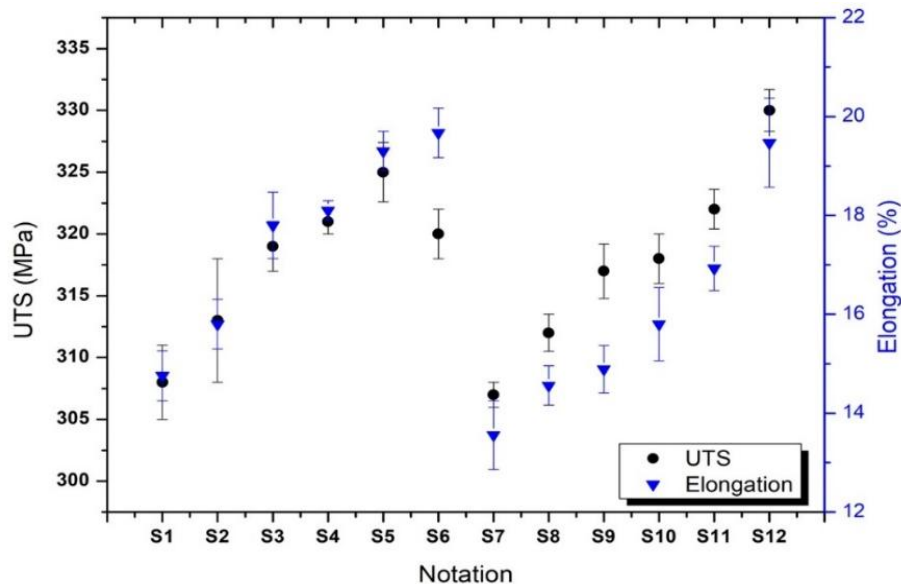


Figure 20. Stress and elongation diagram

A detailed report is generated containing all the observations, the resulting stress-strain curve, and the derived mechanical properties.

#### Conclusion:

It has been established that the friction stir deposition process is a reliable way to create high-performance composites. The exceptional metallurgical and mechanical properties of the composite were attained through a methodical layer-by-layer deposition. From this research, we can infer the following major points:

1. SEM research confirmed that a more uniform distribution of the composite material was achieved when the consumable rod was built and took Ø4 no. of sample rods of  $\text{TiB}_2$  and  $\text{Y}_2\text{O}_3$ .

2. According to the microstructural study of the deposited composite, equiaxed tiny grains are present throughout. This points to dynamic recrystallization happening during the deposition phase, which is crucial in improving the material's initial characteristics.
3. Notably, prolonged plateau stress was seen in composites made of  $\text{TiB}_2$  and  $\text{Y}_2\text{O}_3$  design. This is because the material has the ideal pore size to disperse energy slowly over time, increasing its toughness.
4. The hardness first rises with the addition of more  $\text{TiB}_2$  and  $\text{Y}_2\text{O}_3$  at  $\phi 4$ . Once a specific concentration is reached, however, adding more  $\text{TiB}_2$  and  $\text{Y}_2\text{O}_3$  causes the hardness to drop. This suggests that  $\text{TiB}_2$  and  $\text{Y}_2\text{O}_3$  need to be carefully calibrated when added in order to attain optimal material characteristics, such as maximum hardness.

Overall, this study's findings highlight the promise of the friction stir deposition method for making high-quality composites, as well as in both design and execution that determine the final material's features.

#### Future and scope:

Few articles have compared the influence of various filling procedures on the attributes of the formed surface composite. Also, research in this area is essential for bringing this technique to an industrial level. Compositing characteristics that affect surface composite quality must also be studied. The process of filling Al composite mixtures must be automated and straightforward to facilitate high volumes of composite production. The created composite must be tested for a variety of other properties, such as fatigue and impact resistance.

#### References:

- [1] D.M. Aylor, Metals Handbook V-13, vol. 9, ASM Metals Park, OH, 1982, pp. 859–863.
- [2] S.V. Prasad, P.K. Rohatgi, Tribological properties of Al alloy particle composite, J. Metall. 39 (1987) 22
- [3] R.A. Wang, H.J. Rack, Transition wear behavior of SiC particulate and SiC whisker reinforced 7091 Al metal matrix composite, Mater. Sci. Eng. A 147 (1991) 211–224
- [4] Padmanabham, K.C.A.; Mruthunjaya, M.; Shivakumar, B.P.; Yogesha, K.B.; Siddappa, P.N. Microstructure studies and mechanical characterization of T6 heat treated aluminum and copper-based alloy reinforced with zircon and graphite composite. J. Eng. Sci. Technol. 2019, 14, 2063–2073.
- [5] Joseph, O.O.; Babaremu, K. Agricultural Waste as a Reinforcement Particulate for Aluminum Metal Matrix Composite (AMMCs): A Review. Fibers 2019, 7, 33.
- [6] Gurusamy, P.; Prabu, S.B.; Paskaramoorthy, R. Influence of Processing Temperatures on Mechanical Properties and Microstructure of Squeeze Cast Aluminum Alloy Composites. Mater. Manuf. Process. 2014, 30, 367–373.
- [7] Aybarc, U.; Dispinar, D.; Seydibeyoglu, M.O. Aluminum metal matrix composites with SiC,  $\text{Al}_2\text{O}_3$  and grapheme—Review. Arch. Foundry Eng. 2018, 18, 5–10.
- [8] Purohit, R.; Qureshi, M.; Rana, R. The Effect of Hot Forging and Heat Treatment on Wear Properties of Al6061- $\text{Al}_2\text{O}_3$  Nano Composites. Mater. Today Proc. 2017, 4, 4042–4048.
- [9] Ramkumar, K.; Natarajan, S. Effects of  $\text{TiO}_2$  nanoparticles on the microstructural evolution and mechanical properties on accumulative roll bonded Al nanocomposites. J. Alloy. Compd. 2019, 793, 526–532.
- [10] Gowrishankar, T.P.; Manjunatha, L.H.; Sangmesh, B. Mechanical and Wear behavior of Al6061 reinforced with Graphite and TiC Hybrid MMCs. Mater. Res. Innov. 2019, 24, 179–185.
- [11] Devaraju, A.; Kumar, A.; Kotiveerachari, B. Influence of addition of Grp/ $\text{Al}_2\text{O}_3$  with SiCp on wear properties of aluminum alloy 6061-T6 hybrid composites via friction stir processing. Trans. Nonferrous Met. Soc. China 2013, 23, 1275–1280.



- [12] Soleymani, S.; Abdollah-Zadeh, A.; Alidokht, S. Microstructural and tribological properties of Al5083 based surface hybrid composite produced by friction stir processing. *Wear* 2012, 278–279, 41–47.
- [13] Gandra J, Krohn H, Miranda RM, et al. Friction surfacing—a review. *J Mater Process Technol.* 2014;214(5):1062–1093.
- [14] Bitola R, Pandit D, Pratap C, et al. Two decades of friction stir processing—a review of advancements in composite fabrication. *J Adhes Sci Technol.* 2022;36(8):795–832.
- [15] Heidarzadeh A, Mironov S, Kaibyshev R, et al. Friction stirs welding/processing of metals and alloys: a comprehensive review on microstructural evolution. *Prog Mater Sci.* 2021; 117:100752.
- [16] Sakihama H, Tokisue H, Katoh K, et al. Mechanical properties of a friction-surfaced 5052 aluminum alloy. *J. Japan Inst. Light Metals.* 2002;52(8):346–351.
- [17] Gandra J, Vigarinho P, Pereira D, et al. Wear characterization of functionally graded Al–SiC composite coatings produced by friction surfacing. *Materials & Design (1980- 2015).* 2013; 52:373–383.
- [18] Karthik GM, Ram GJ, Kottada RS, et al. Friction deposition of titanium particle-reinforced aluminum matrix composites. *Materials Science and Engineering: A.* 2016;653: 71–83.
- [19] Shinoda T, Okamoto S, Takemoto S, et al. Deposition of hard surfacing layer by friction surfacing. *Weld Int.* 1996;10(4):288–294.
- [20] Awasthi, A.; Panwar, N.; Wadhwa, A.S.; Chauhan, A. Mechanical Characterization of hybrid aluminum composite-a review. *Mater. Today Proc.* 2018, 5, 27840–27844.
- [21] Gandra J, Vigarinho P, Pereira D, et al. Wear characterization of functionally graded Al–SiC composite coatings produced by friction surfacing. *Materials & Design (1980- 2015).* 2013; 52:373–383.
- [22] Karthik GM, Ram GJ, Kottada RS, et al. Friction deposition of titanium particle-reinforced aluminum matrix composites. *Materials Science and Engineering: A.* 2016;653: 71–83.
- [23] Reddy GM, Rao KS, Mohandas T, et al. Friction surfacing: a novel technique for metal matrix composite coating on aluminum–silicon alloy. *Surf Eng.* 2009;25(1):25–30.
- [24] Shinoda T, Okamoto S, Takemoto S, et al. Deposition of hard surfacing layer by friction surfacing. *Weld Int.* 1996;10(4):288–294.
- [25] Gandra J, Pereira D, Miranda RM, et al. Deposition of AA6082-T6 over AA2024-T3 by friction surfacing-mechanical and wear characterization. *Surf Coat Technol.* 2013;223: 32–40.
- [26] Bedford GM, Vitanov VI, Voutchkov II, et al. On the thermo-mechanical events during friction surfacing of high-speed steels. *Surf Coat Technol.* 2001;141(1):34–39.
- [27] Suhuddin U, Mironov S, Krohn H, et al. Microstructural evolution during friction surfacing of dissimilar aluminum alloys. *Metal and Mat Trans A.* 2012;43(13):5224–5231.
- [28] Baradeswaran, A.; Perumal, A.E. Study on mechanical and wear properties of Al 7075/Al<sub>2</sub>O<sub>3</sub>/graphite hybrid composites. *Compos. Part B Eng.* 2014, 56, 464–471.
- [29] Sharifi, E.M.; Karimzadeh, F. Wear behavior of aluminum matrix hybrid nanocomposites fabricated by powder metallurgy. *Wear* 2011, 271, 1072–1079.
- [30] Ravindran, P.; Manisekar, K.; Narayanasamy, P.; Selvakumar, N. Application of factorial techniques to study the wear of Al hybrid composites with graphite addition. *Mater. Des.* 2012, 39, 42–54.
- [31] Suresha, S.; Sridhara, B. Wear characteristics of hybrid aluminum matrix composites reinforced with graphite and silicon carbide particulates. *Compos. Sci. Technol.* 2010, 70, 1652–1659.

- [32] Srinivasan, R.; Shrinivasan, B.H.; Prasath, K.J.; Saleth, R.J.; Anandhan, R. Experimental investigation of aluminum hybrid metal matrix composites processed through squeeze casting process. *Mater. Today Proc.* 2020, 27, 1821–1826
- [33] M. Engineering, investigation of single-pass/double-pass techniques on friction stir welding of aluminum, *J. Mech. Eng. Sci.* 7 (December) (2014) 1053–1061.
- [34] M.M. El-rayes, E.A. El-danaf, the influence of multi-pass friction Stir on the microstructural and mechanical properties of Aluminum alloy 6082, *J. Mater. Process. Technol.* 212 (5) (2012) 1157–1168.